

## RESEARCH PAPER

## PREDICTION THERMO-PHYSICAL CHARACTERISTICS HEAT-RESISTANT NICKEL ALLOYS DIRECTIONAL CRYSTALLIZATION

Alexander Anatolyevich Glotka<sup>1\*</sup>, Vadim Efimovich Ol'shanetskii<sup>1</sup><sup>1</sup> Zaporizhzhia Polytechnic National University, Ukraine, Zaporizhzhia, st. Zhukovskogo, 64, 69063

\*Corresponding author: glotka-alexander@ukr.net, tel.: +380964275651, Zaporizhzhia Polytechnic National University, Ukraine, Zaporizhzhia, st. Zhukovskogo, 64, 69063

Received: 11.01.2021

Accepted: 31.01.2021

## ABSTRACT

The paper presents a comparative analysis of the practical and calculated values of the thermophysical properties of heat-resistant nickel alloys of directional solidification. Using an empirical approach, new ratios of the elements  $K\gamma'$  and  $K\gamma$  have been obtained for the first time, which take into account the combined effect of alloying elements on the temperature of multicomponent compositions of cast heat-resistant alloys. The calculated values of the critical temperatures for the Ni-6Al-9Co-8W-4Re-4Ta-1.5Nb-1Mo-0.15C system are in good agreement with the experimental ones. The dependence of the  $K\gamma$  ratio on the alloying system; the influence of alloying on the liquidus temperature of the alloys is studied. The ratios of the content of alloying elements and regression models that can be used to predict the width of the crystallization temperature range and the optimal homogenization temperature for a particular alloy are presented.

**Keywords:** casting heat-resistant nickel alloys directional solidification, thermodynamic processes phase separation, critical temperatures

## INTRODUCTION

In recent years, the development of jet aircraft, the temperature of the hydrogen-containing gas at the turbine inlet has increased from 1200 K in the second-generation engines to 1800-1950 K in the fifth-generation engines. About 70% of this increase was obtained due to the improvement of air-cooling systems for gas turbine blades, and 30% - as a result of an increase in the level of mechanical properties of heat-resistant nickel alloys (HRNA) [1 - 5].

The main thermophysical and structural-phase characteristics that determined the choice of the most promising compositions of the developed alloys were the temperatures: complete dissolution of the  $\gamma'$ -phase in the matrix  $\gamma$ -solid solution  $t_{c,d}$  (solvus  $\gamma'$ ), local melting of the nonequilibrium eutectic (peritectic)  $\gamma + \gamma'$ , solidus  $t_s$  and liquidus  $t_L$ . The achievement of the maximum values these temperatures (thermodynamic stability of the phases) determines the high temperature performance and creep resistance of the HRNA [6-9]. It should be noted that while striving to increase the critical temperatures  $t_{c,d}$ ,  $t_{eut}$ ,  $t_s$  and  $t_L$ , it is necessary to provide a sufficient temperature interval - ( $t_{eut} - t_{c,d}$ ) to eliminate the risk of melting during homogenizing annealing [10-15].

As a result of this empirical approach, heat-resistant nickel alloys are the most complex alloys for structural purposes, since they contain more than 15 alloying and microalloying elements. Currently, with alloys of this class, tests are being carried out to optimize the chemical composition, which will make it possible to obtain the required set of properties [16-23].

The purpose of this work is to obtain predictive regression models, with the help of which, it is possible to adequately

calculate the critical temperatures for the HRNA directional crystallization, without conducting preliminary experiments.

## MATERIAL AND METHODS

For experimental and theoretical studies of temperature performance, a working sample of alloys was formed, consisting of well-known industrial HRNA for directional crystallization of domestic and foreign production, the following brands: ZhS-26, ZhS-26U, ZhS6F, ZhS-28, ZhS-30, VZhL-20, GTD-111, Mar-M247, CM-247LC, Mar-M200 + Hf, Mar-M246 + Hf, U-500, U-700, PWA-1422, PWA-1426, CM-186LC, Rene 142, Rene 150, IN-792LC, DS-16, Mar-M002, Rene 125, Rene 80H. The selection of alloys was made from the standpoint of a variety of chemical compositions (alloying systems), which have a wide alloying range in terms of the content of the main elements.

The obtained values were processed in the Microsoft Office software package in the EXCEL package to obtain correlation dependences of the "parameter-property" type with obtaining mathematical equations of regression models that optimally describe these dependences. The dependences have a sufficiently high coefficient of determination  $R^2 \geq 0.85$  and are suitable for determining the temperature characteristics of the HRNA.

## RESULTS AND DISCUSSION

The heat resistance of alloys is determined by the thermodynamic stability of the phases, which is proposed to be estimated by the temperatures  $t_{c,d}$ ,  $t_{eut}$ ,  $t_s$ , and  $t_L$ . Development of a method for calculating these values from the chemical composition of the alloy is an urgent task.

All components used for alloying HRNA can be conditionally divided into three groups: dissolving mainly in the  $\gamma$ -solid solution (Co, Cr, Mo, W, Re), dissolving mainly in the  $\gamma'$ -phase (Al, Ti, Ta, Hf) and carbide-forming elements (Ti, Ta, Hf, Nb, V, W, Mo, Cr).

On the other hand, many elements can be included in the  $\gamma'$ -phase: Al, Ti, Nb, Cr, Co, Mo, W, V, etc. But their content in the  $\gamma'$ -phase and the effect on its amount in the structure are different. This effect is associated with the ability of the elements to form stable intermetallic phases of the  $Ni_3Me$  type with nickel. Hence, it follows that the critical temperatures of alloys are influenced not only by the elements that belong to  $\gamma'$ -forming, but also those that are classified as  $\gamma$ -solid hardeners. As a result of processing the experimental data and the above reasoning, the relationship

$$K_{\gamma'} = 5 \frac{\sum_{\gamma'} (Al+Ti+Nb+Ta+Hf) \text{ elements to assess the}}{\sum_{\gamma} (Cr+W+Mo+Re+Co+Ru)}$$

thermodynamic stability of phases, which takes into account the complex effect of all alloy components. This ratio correlates well with the temperatures  $t_{c,d}$ ,  $t_{eut}$  and  $t_s$ ,  $\Delta t_{homo}$ , °C which, in turn, correlate well with the heat resistance of the alloys. Also, this ratio can be used in the design of other types of heat-resistant nickel-based alloys [24].

The relationship between the temperatures of complete dissolution of the  $\gamma'$ -phase, eutectic transformation and solidus with the proposed  $K_{\gamma'}$  ratio (Fig. 1) is adequately described by regression models (Table 1). An increase in the thermophysical characteristics of alloys with an increase in the parameter  $K_{\gamma'}$  is associated with an increase in alloying of the alloys with both  $\gamma$ -forming elements and elements in the  $\gamma$ -solid solution. However, at a value of 1.6 ... 1.7  $K_{\gamma'}$ , a decrease in temperatures  $t_{c,d}$  and  $t_s$  is observed, due to the peculiarities of alloying in this range, namely, an increase in the content of elements that are classified as  $\gamma$ -hard mortar hardeners. With an increase in the value over 2.2 ... 2.3  $K_{\gamma'}$ , an increase in the temperatures  $t_{c,d}$  and  $t_s$  is observed, which is associated with a change in the interatomic bond forces (due to an increase in alloying alloying).

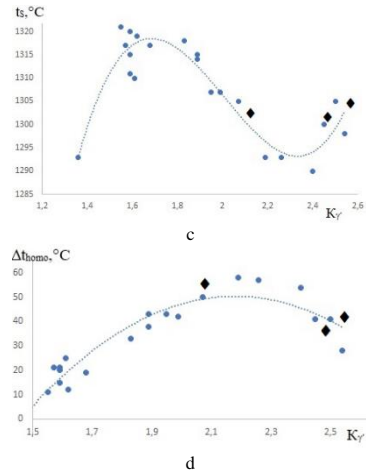
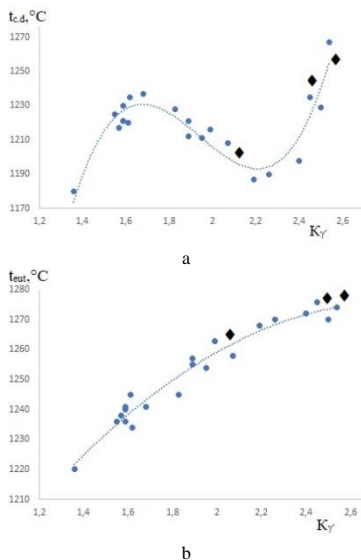


Fig. 1. - Dependence critical temperatures and homogenization interval on the ratio alloying elements in the composition of the HRNA: a -  $t_{c,d}=f(K_{\gamma'})$ ; b -  $t_{eut}=f(K_{\gamma'})$ ; c -  $\Delta t_{homo}=f(K_{\gamma'})$ ; d -  $t_s=f(K_{\gamma'})$ . (•- calculated values; ♦ - experimental values)

Using the constructed regression models (Table 1), it is possible to predict with high accuracy the critical temperatures of alloys without preliminary experiments by the method of differential thermal analysis, and also to calculate the width of the temperature range for efficient homogenizing annealing depending on the content of alloying elements in the alloy.

Table 1 Dependences of the thermophysical characteristics of the liquid pumping station on the parameters  $K_{\gamma'}$  and  $K_{\gamma}$ .

Critical temperature	Predictive regression models
Temperatures of complete dissolution of the $\gamma'$ -phase	$t_{c,d}=504,84(K_{\gamma'})^3-2942,7(K_{\gamma'})^2+5611,1(K_{\gamma'})-2284,3$
Temperature of eutectic transformation $\gamma + \gamma'$	$t_{eut}=-26,039(K_{\gamma'})^2+145,92(K_{\gamma'})+1071,5$
Temperature range for homogenizing annealing	$\Delta t_{homo}=-97,465(K_{\gamma'})^2+424,79(K_{\gamma'})-412,46$
Solidus temperature	$t_s=186,75(K_{\gamma'})^3-1125,5(K_{\gamma'})^2+2202,4(K_{\gamma'})-90,528$
Liquidus temperature	$t_L=-10,235(K_{\gamma'})^2+75,121(K_{\gamma'})+1234,1$
Crystallization temperature range	$\Delta t_{cryst}=49,07(K_{\gamma'})^3-318,68(K_{\gamma'})^2+978,96(K_{\gamma'})-777,42$

However, the relationship between the  $K_{\gamma'}$  ratio and the liquidus temperature turned out to be ambiguous. The initial dependence had a low coefficient of determination ( $R^2 \leq 0.1$ ). This is explained by the fact that at temperatures close to the melting point, there are two phases in the structure, a liquid and  $\gamma$ -solid solution. The liquidus temperature is associated with the thermodynamic stability of the solid solution, which is influenced by the refractory elements in it, they dissolve mainly in the  $\gamma$ -solid solution and significantly increase the thermodynamic stability of the phases in the HRNA due to the low diffusion coefficient, which leads to inhibition of the mobility of atoms in  $\gamma$ - phase. Therefore, after processing the experi-

mental data, and following the above judgments, the following ratio of elements was proposed for the first time:

$$K_{\gamma} = \frac{\sum_{\gamma} (Cr+W+Mo+Re+Co+Ru)}{\sum_{\gamma} (Al+Ti+Nb+Ta+Hf)}$$

possible to accurately predict the liquidus temperature and the temperature range of the HRNA crystallization [24].

Figure 2 shows the dependences of the liquidus temperature and the crystallization interval on the  $K_{\gamma}$  ratio. The liquidus temperature increases with an increase in the value of  $K_{\gamma}$ , which is typical with an increase in elements that are in a solid solution. The dependence of the temperature range of crystallization on the value of  $K_{\gamma}$  has a similar character with  $t_{c,d}$  and  $t_s$  and obeys the above relationships.

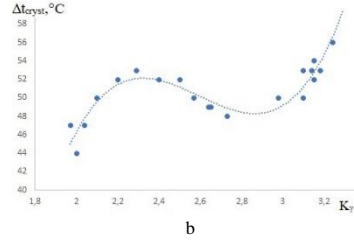
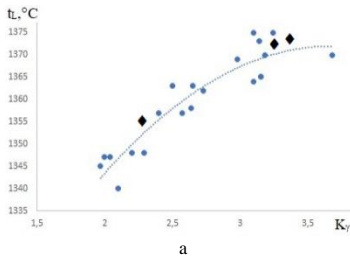


Fig. 2. - Dependence of the liquidus temperature (a) and the crystallization interval (b) on the  $K_{\gamma}$  ratio. (• - calculated values; ♦ - experimental values)

Thus, using the above regression models (Table 1), it is possible to calculate the liquidus temperature and the width of the crystallization temperature range, which significantly affects the manufacturability of the alloy during the formation of a defect-free structure in castings.

The results of calculating the thermophysical characteristics of the directed crystallization HRNA were further compared with the experimental data obtained using differential thermal analysis (DTA). To confirm the calculated data, industrial high-temperature nickel alloys of the Ni-6Al-9Co-8W-4Re-4Ta-1.5Nb-1Mo-0.15C system (ZhS32-VI, ZhS32B-VI and ZhS32E-VI) were selected. Based on the analysis of the experimentally obtained data on the critical temperatures of phase transformations on the experimental alloys, Table 2 presents the values of the calculated thermophysical characteristics obtained using an active experiment.

Table 2 Calculated and experimental thermophysical characteristics HRNA

Method of obtaining results	Critical temperatures, °C					
	$t_{c,d}$	$t_{eut}$	$t_s$	$t_L$	$\Delta t_{homo}$	$\Delta t_{cryst}$
<b>ZhS32-VI</b>						
Calculated	1205	1265	1303	1355	55	53
Experimental	1197	1260	1298	1352	48	54
<b>ZhS32B-VI</b>						
Calculated	1250	1273	1302	1372	31	70
Experimental	1230	1270	1296	1368	40	72
<b>ZhS32E-VI</b>						
Calculated	1261	1278	1306	1376	37	69
Experimental	1250	1271	1297	1367	35	70

Table 2 shows that the calculated and experimental data are in good agreement with each other in almost all characteristics. Based on the calculated and experimental values obtained, the error does not exceed 15°C, thus, the obtained mathematical dependences make it possible to predict the thermophysical characteristics, which depend on the alloying system of the alloy, both in the development of new compositions of the HRNA for directional crystallization, and in the improvement of known industrial compositions within the brand composition.

## CONCLUSION

1. On the basis of an integrated approach, both computational and experimental, for multicomponent liquid pumping stations, new regression models have been obtained that make it possible to adequately predict the thermophysical characteristics by the chemical composition of the alloy. On the basis of the thermodynamic approach, new ratios of  $K_{\gamma'}$  and  $K_{\gamma}$  have been

obtained for the first time; by their value, one can adequately predict the temperature characteristics for multicomponent compositions of directional crystallization of HRNA.

2. The dependences of the ratio of  $K_{\gamma'}$  to the temperatures of complete dissolution of the  $\gamma'$  phase, eutectic transformation and solidus have been revealed; they are explained by the connection between alloying of the alloy with  $\gamma'$ -forming elements, and being in the  $\gamma$ -solid solution.

3. It has been established that the liquidus temperature increases with an increase in the value of  $K_{\gamma}$ , which is typical with an increase in elements that are in a solid solution. The dependence of the temperature range crystallization on the value of  $K_{\gamma}$  has a similar character with  $t_{c,d}$  and  $t_s$ .

4. The results obtained show that the ratios of such a group of elements practically unidirectionally affect the diagrams (behavior of figurative points of state diagrams from virtual alloys) of the considered heat-resistant alloys. Good agreement between the calculated and experimental results made it possible to believe that the "intersection" of multidimensional

parabolas of various hypersurfaces of phase equilibria makes it possible to obtain a binary section of conditional equilibrium diagrams with lines of equilibrium phases corresponding to physical reality.

5. A promising and effective direction is shown in solving the problem of predicting the thermodynamic stability of alloy phases, which affects the service properties of alloys both in the development of new HRNA and in the improvement of the compositions of well-known industrial brands of this class.

## REFERENCES

1. B. G. Choi, I. S. Kim, D. H. Kim, C. Y. Jo: Solid State Phenomena, 124–126, 2007, S1505–1508. <https://doi.org/10.4028/www.scientific.net/ssp.124-126.1505>.
2. M. Kvapilova, J. Dvorak, P. Kral, K. Hrbacek, V. Sklenicka: High Temperature Materials and Processes, 38, 2019, 590–600. <https://doi.org/10.1515/htmp-2019-0006>.
3. N. V. Petrushin, E. S. Elyutin, R. M. Nazarkin, S. I. Pakhomkin, V. G. Kolodochkina, T. V. Fesenko, E. S. Dzhi-oeva: Inorg. Mater. Appl. Res., 7, 2016, 824–831. <https://doi.org/10.1134/S2075113316060149>.
4. S. M. Seo, I. S. Kim, J. H. Lee, C. Y. Jo, H. Miyahara, K. Ogi: Metall. Mater. Trans. A, 38, 2007, 883–893. <https://doi.org/10.1007/s11661-007-9090-0>.
5. O. I. Balyts'kyi, O. O. Krokhmal'nyi: Mater. Sci., 35, 1999, 389–394. <https://doi.org/10.1007/BF02355483>.
6. A. M. S. Costa, E. S. N. Lopes, R. J. Contieri, R. Caram, R. Baldan, G. E. Fuchs, et al: J. Mater. Eng. Perform, 28, 2019, 2427–2438. <https://doi.org/10.1007/s11665-019-04014-1>.
7. Yu. A. Bondarenko, A. B. Echin, V. E. Bazhenov, A. V. Kolytgin: Russian Journal of Non-ferrous Metals, 58, 2017, 481–488. <https://doi.org/10.3103/S1067821217050042>.
8. A. Balyts'kyi: 6th International Conference “Fracture Mechanics of Materials and Structural Integrity”, 16, 2019, 134–140. <https://doi.org/10.1016/j.prostr.2019.07.032>.
9. N. Das: Trans. Indian. Inst. Met., 63, 2010, 265–274. <https://doi.org/10.1007/s12666-010-0036-7>.
10. K. Mukai, Z. Li, K. C. Mills: Metall. Mater. Trans. B, 36, 2005, 255–262. <https://doi.org/10.1007/s11663-005-0027-y>.
11. Z. Li, K. C. Mills: Metall. Mater. Trans. B 37, 2006, 781–790. <https://doi.org/10.1007/s11663-006-0060-5>.
12. J. Huang, X. Yang, D. Shi, H. Yu, X. Hu: J. Mater. Sci., 49, 2014, 7625–7638. <https://doi.org/10.1007/s10853-014-8418-6>.
13. L. Li, A. Deceuster, C. Zhang: Metallogr. Microstruct. Anal., 1, 2012, 92–98. <https://doi.org/10.1007/s13632-012-0016-x>.
14. M. Z. Alam, N. Hazari, D. K. Das: Bull. Mater. Sci., 37, 2014, 1551–1561. <https://doi.org/10.1007/s12034-014-0110-6>.
15. Yu. H. Kvasnytska, L. M. Ivaskevych, O. I. Balytskyi, I. I. Maksyuta, H. P. Myalnitsa: Mater. Sci., 56, 2020, 432–440. <https://doi.org/10.1007/s11003-020-00447-5>.
16. L. Li: J. Mater. Sci., 41, 2006, 7886–7893. <https://doi.org/10.1007/s10853-006-0948-0>.
17. O. A. Glotka, S. V. Haiduk: Metallofiz. Noveishie Tekhnol., 42(6), 2020, 869–884 (in Russian) <https://doi.org/10.15407/mfint.42.06.0869>.
18. J. Song, D. Tang, C. Xiao, D. Wang, Q. Yu: Rare Metals, 30, 2011, 383–387. <https://doi.org/10.1007/s12598-011-0308-3>.
19. M. Suave, L. Muñoz, A. S. Gaubert: Metall. Mater. Trans. A, 49, 2018, 4012–4028. <https://doi.org/10.1007/s11661-018-4708-y>.
20. O. N. Senkov, D. W. Mahaffey, S. L. Semiatin: Metall. Mater. Trans. A, 45, 2014, 5545–5561. <https://doi.org/10.1007/s11661-014-2512-x>.
21. J. Zhang, R. F. Singer: Metall. Mater. Trans. A, 35, 2004, 1337–1342. <https://doi.org/10.1007/s11661-004-0308-0>.
22. H. Y. Qi, J. S. Yang, X. G. Yang, L. Shao-Lin: Rare Metals, 38, 2019, 227–232. <https://doi.org/10.1007/s12598-016-0862-9>.
23. A. A. Glotka, S. V. Gaiduk: J Appl Spectrosc, 87, 2020, 812–819. <https://doi.org/10.1007/s10812-020-01075-2>.
24. A. A. Hlotka, S. V. Haiduk: Mater. Sci., 55, 2020, 878–883. <https://doi.org/10.1007/s11003-020-00382-5>.